ON THE INTENSITY AND POLARISATION OF THE LIGHT FROM THE SKY DURING TWILIGHT—PART II

By J. V. Dave
(*Physical Research Laboratory, Ahmedabad-9*)

Received April 12, 1956
(Communicated by Professor K. R. Ramanathan, F.A.SC.)

I. Introduction

In a recent paper,[1] observations of the intensity and polarisation of the light from the sky during twilight taken at Mount Abu during 1951 were presented and briefly discussed. It was shown that for depressions of the sun exceeding 7° or 8°, the zenith sky was much brighter than would be expected if primary scattering alone were responsible for the light and that in the treatment of twilight problems, due account should be taken of the contributions from secondary scattering, as has been shown by Hulburt.[2] Marked discontinuities in the polarisation of the light from the zenith sky at solar depressions of 5°, 8°, 12° and 17° support the presence in twilight of other contributions in addition to primary scattered light.

1.1. *Summary of previous work*

Robley[3] has recently given a method of calculating the intensity and polarisation of the secondary (multiply) scattered light during twilight. His work is based on the work of Dr. S. Chandrasekhar[4] for an infinite plane-parallel atmosphere of defined optical thickness. To compute the secondary scattered radiation for the zenith sky for a solar depression D, Robley extends the atmospheric path traversed by the solar rays to a vertical plane in the atmosphere passing through the centre of the earth and making an angle D/2 with the observer's vertical. He then calculates the scattered light emanating from this plane in a direction parallel to the observer's horizon, with certain simplifying assumptions which lead to a constant value of 50% for the polarisation of the secondary scattered light from the zenith sky throughout the period of twilight. *Prima facie*, this does not appear to be correct, because observation shows that with increasing values of solar depression, the brightness of the sky becomes more and more concentrated towards the horizon in the sun's meridian plane.

1.2. *General outline of the method adopted in this paper*

The method adopted in this paper for the calculation of secondary scattering is based on the work of Chapman and Hammad.[5,6] The following assumptions were made:—

(1) The earth was taken to be a uniform sphere of radius 6370 km., surrounded by an exponential atmosphere of equivalent scale height 7 km.

(2) The atmosphere was arbitrarily divided into a number of concentric shells of 4 km. thickness, for computing the intensities of primary and secondary scattered radiations.

(3) The solar radiation falling on the top of the atmosphere was assumed to be unpolarised and its intensity taken to be unity.

(4) The depolarisation factor d of air due to molecular anisotropy was taken to be 0·04.

(5) Higher orders of scattering than secondary were neglected.

(6) No correction was made for the absorption or scattering of light by dust or haze.

(7) Atmospheric refraction was neglected.

(8) No correction was made for reflection by the ground.

II. THEORY

In Fig. 1, ABC represents a section of the earth; O is its centre and a its radius. R_0 is the position of the observer on the surface of the earth. OR_0 represents the direction of the observer's zenith. Q is a point in the atmosphere in the direction of observation R_0Q. The Z-axis is chosen to lie along the observer's zenith OR_0. The X-axis lies in the plane of the paper such that the XOZ plane is parallel to the incident solar radiation. The Y-axis is perpendicular to the plane of paper passing through O. The polar co-ordinates (θ, ϕ) of a given direction are such that θ is the angle which the direction makes with the Z-axis; and ϕ is the azimuth with XOZ as the reference plane. With this convention, the polar co-ordinates of the incident solar radiation SP are (Z_0, O). If the direction of observation is the zenith or R_0Q, its θ, ϕ are (O, O). PQ the direction of primary scattered radiation is given by (θ', ϕ'). The unit vectors along SP, QR_0 and PQ are denoted respectively by s, k and k'.

2.1. *Intensity of primary scattered radiation*

Consider a solar beam of intensity I_∞ travelling along SP. I_∞ denotes the intensity of solar radiation outside the earth's atmosphere in a specified narrow wave band, being the energy received per unit time on unit area normal to the vector s. Let σ denote the mass coefficient of scattering and ρ the density of air at a distance s from P along PS.

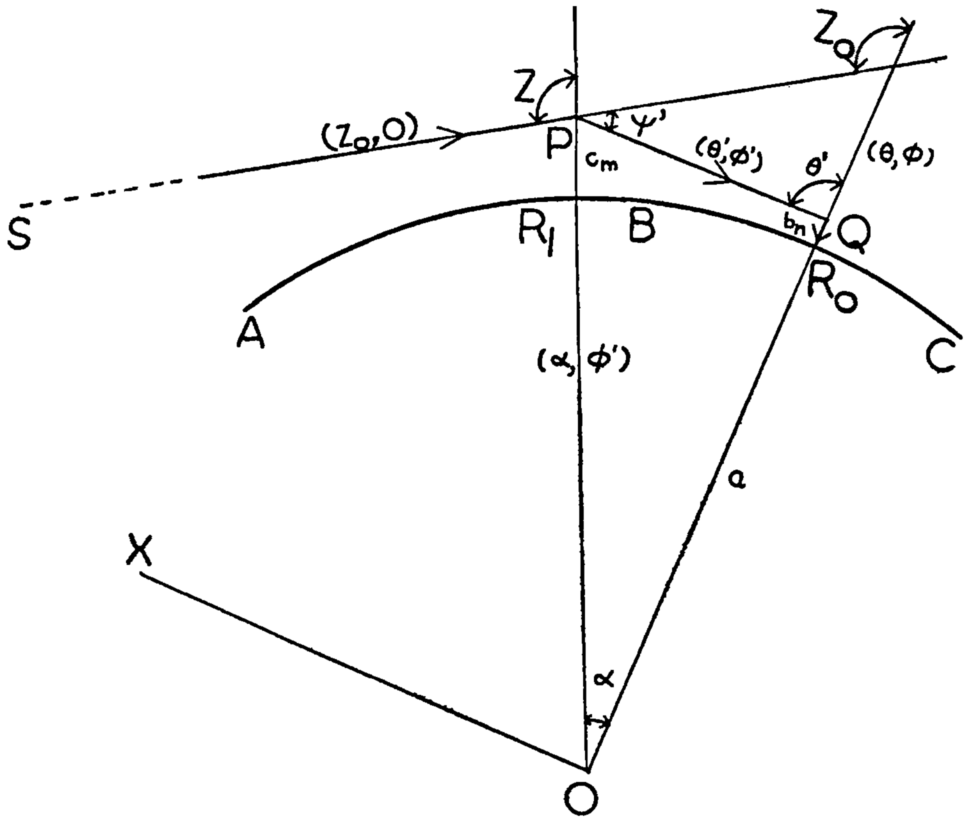

FIG. 1. The incident light is primarily scattered at P (where the local zenith angle of the sun is Z, and the height $R_1P = c_m$). The direction PQ is defined by (θ', ϕ'). The direction of observation towards the observer's zenith is defined by $\theta = 0$, $\phi = 0$. The primary scattered light travelling along PQ gets rescattered at Q along QR_0 towards the observer. $QR_0 = b_n$.

Then

$$\int_{\infty}^{P} \sigma \cdot \rho \cdot ds = \tau_{SP} \tag{1}$$

is the equivalent optical path which the solar radiation has to travel in the earth's atmosphere before reaching P. It will be shown later that τ_{SP} is a function of the vertical height c_m of P above the surface of the earth and of the local zenith angle (Z) of the sun at P. The intensity of the solar radiation at P is then given by

$$I = I_{\infty} \cdot e^{-\tau_{SP}} \tag{2}$$

Let PQ (θ', ϕ') be a direction along which the incident solar radiation is scattered from P according to the Rayleigh law of scattering. The energy scattered from P in a cone of small solid angle dk' with apex at P is given by

$$E_1\, dk' = \frac{3\sigma I_\infty}{16\pi\,(1 + \frac{1}{2}d)}\, e^{-\tau_{SP}}\, (1 + \cos^2\psi' + d\sin^2\psi')\, dk' \qquad (3)$$

where d is the depolarisation factor due to molecular anisotropy and ψ' the angle between s and k' given by

$$\cos\psi' = \cos Z_0 \cos\theta' + \sin Z_0 \sin\theta' \cos\phi' \qquad (4)$$

This scattered radiation is polarised and can be resolved into two beams of plane polarised light at right angles to each other. If $E_{1n'}$ represents the primary scattered emission from P in the direction of k' with its electric vibration along the vector n' perpendicular to the plane sk' at P, and $E_{1t'}$, the intensity of the radiation with its electric vector along t' perpendicular to n', we have

$$E_{1n'} = \frac{3\sigma I_\infty}{16\pi\,(1 + \frac{1}{2}d)}\, e^{-\tau_{SP}} \qquad (5)$$

and

$$E_{1t'} = KE_{1n'} \qquad (6)$$

where

$$K = d + (1 - d)\cos^2\psi' \qquad (7)$$

Consider a small surface area dS at Q perpendicular to PQ. The amount of primary scattered radiation from P passing through dS per second is given by

$$E_{1n'}\,(1 + K)\, e^{-\tau_{PQ}} \times \frac{dS}{s^2}$$

where dS/s^2 is the solid angle subtended by dS at P and τ_{PQ} the equivalent optical path from P to Q. It will be later shown that τ_{PQ} which is given by

$$\tau_{PQ} = \int_P^Q \sigma \cdot \rho \cdot ds$$

is a function of θ', c_m and b_n. If dV is a small volume element surrounding P and subtending a small solid angle dk' at dS, and if ρ' is the density at P, then the amount of primary scattered radiation passing through dS per second from a mass element $\rho' \cdot dV$ surrounding P is given by

$$E_{1n'}\,(1 + K)\, e^{-\tau_{PQ}} \frac{dS}{s^2}\, \rho' \cdot dV$$

and the intensities $R_{1n'}$ and $R_{1t'}$ of the normal and transverse components of primary scattered radiation passing normally through unit area at Q through unit solid angle along k' is given by

$$R_{1n'} = \int_{Q}^{\infty} E_{1n'}\, e^{-\tau_{PQ}} \frac{dS}{s^2} \times \frac{\rho' \cdot dV}{dS \cdot dk'}$$

and

$$R_{1t'} = KR_{1n'}$$

the integration extending from ∞ to Q when the whole path is illuminated by solar rays, or upto the shadow limit when a part of PQ lies in the shadow region of the earth.

Substituting the values of $E_{1n'}$ and of $dV = s^2 \cdot ds.dk'$ in $R_{1n'}$, we have

$$R_{1n'} = \frac{3\sigma I_{\infty}}{16\pi(1 + \frac{1}{2}d)} \int_{Q}^{\infty} e^{-\tau_{SP}} e^{-\tau_{PQ}} \rho' . ds \tag{8}$$

and

$$R_{1t'} = KR_{1n'} \tag{9}$$

It must be noted that unlike the plane-parallel atmosphere, cos Z on the actual earth changes along QP and also with ϕ'. Hence τ_{SP} is not independent of ϕ'. Thus the integration formulæ developed by Chapman and Hammad for $R_{1n'}$ are not applicable in this and we have adopted numerical integration.

2.2. *Intensity of secondary scattered radiation*

Having obtained the values of $R_{1n'}$ and $R_{1t'}$ for different values of θ' and ϕ' at Q, the next problem is to consider the effective contribution by the volume element at Q towards the secondary scattered radiation travelling along QR_0. Let n be the unit vector perpendicular to the $k'k$ plane at Q. If E_{2n} and E_{2t} are defined as the energy of the secondary emission for normal and transverse components emitted at Q respectively, then as shown by Hammad, we have

$$E_{2n} = \frac{3\sigma}{16\pi(1 + \frac{1}{2}d)} \int \{A_1 + KA_2\} R_{1n'}\, dk'$$

and

$$E_{2t} = \frac{3\sigma}{16\pi(1 + \frac{1}{2}d)} \int \{B_1 + KB_2\} R_{1n'}\, dk'$$

where

$$\left.\begin{aligned} A_1 &= d + 2\,(1 - d)\cos^2 \chi_{nn'} \\ A_2 &= d + 2\,(1 - d)\cos^2 \chi_{nt'} \\ B_1 &= d + 2\,(1 - d)\cos^2 \chi_{tn'} \\ B_2 &= d + 2\,(1 - d)\cos^2 \chi_{tt'} \end{aligned}\right\} \qquad (10)$$

$\chi_{nn'}$, $\chi_{nt'}$, $\chi_{tn'}$ and $\chi_{tt'}$ are respectively the angles between the vectors n and n', n and t', t and n' and t and t' and the formulæ for obtaining their values are as given by Hammad.

$$\cos \chi_{nn'} = \cos\ (\xi - \xi') \qquad (11)$$

$$\cos \chi_{nt'} = \cos \psi' \sin (\xi - \xi') \qquad (12)$$

$$\cos \chi_{tn'} = \cos \psi \sin (\xi' - \xi) \qquad (13)$$

$$\cos \chi_{tt'} = \sin \psi \sin \psi' + \cos \psi \cos \psi' \cos (\xi' - \xi) \qquad (14)$$

where ψ, ψ', ξ and ξ' are defined by the equations

$$\cos \psi = \cos Z_0 \cos \theta + \sin Z_0 \sin \theta \cos \phi \qquad (15)$$

and

$$\sin \xi = \frac{\sin \theta \sin \phi}{\sin \psi} \qquad (16)$$

Since $dk' = \sin \theta'.d\theta'.d\phi'$, the equations for E_{2n} and E_{2t} can be re-written as

$$E_{2n} = \frac{3\sigma}{16\pi\,(1 + \frac{1}{2}d)} \iint \{A_1 + KA_2\}\, R_{1n'} \sin \theta'.d\theta'.d\phi' \quad (17)$$

and

$$E_{2t} = \frac{3\sigma}{16\pi\,(1 + \frac{1}{2}d)} \iint \{B_1 + KB_2\}\, R_{1n'} \sin \theta'.d\theta'.d\phi' \quad (18)$$

Knowing E_{2n} and E_{2t} for a number of points along QR_0, the tota secondary scattered radiation received at R_0 along QR_0, can be integrated. Its normal and transverse components R_{2n} and R_{2t} are given by

$$R_{2n} = \int_{R_0}^{\infty} E_{2n} e^{-\tau_{QR_0}} \rho . ds \qquad (19)$$

and

$$R_{2t} = \int_{R_0}^{\infty} E_{2t}\, e^{-\tau_{QR_0}} \rho . ds \qquad (20)$$

where ρ is the density of air at Q and τ_{QR_0} is the equivalent optical path from Q to R_0. It is a function of b_n as well as of θ.

III. TABLES FOR COMPUTING THE SECONDARY SCATTERED RADIATION

The quantities required for computing $R_{1n'}$ by the summation method such as s, Δs, τ_{SP}, have been tabulated by many workers such as Sekera,[7] Chapman[8,9] and others. However, their tabulation could not easily fit into our system, and all the quantities required for this work were therefore tabulated from the formulæ given below.

As already mentioned in 1.2, the atmosphere is arbitrarily divided into a number of concentric layers of 4 km. thickness. The base of the nth layer is at a height of $4(n-1)$ km. while its centre is at $(4n-2)$ km. The positions of Q are selected at the base of the different layers, and of P at the centres of the successive layers. On replacing the integral of Equation (8) by a sum, we have

$$R_{1n'} = \frac{3\sigma\rho_0 I_\infty}{16\pi(1+\frac{1}{2}d)} \sum e^{-\tau_{SP}} e^{-\tau_{PQ}} e^{-c_m/H} \Delta s \tag{21}$$

$\rho' = \rho_0 e^{-c_m/H}$ for an exponential atmosphere and H the equivalent scale height is assumed to have a uniform value of 7 km.

If the values of τ_{SP}, τ_{PQ} at the centres of the different layers and also of Δs the thickness of the layers for any θ' are known, $R_{1n'}$ can be calculated. Since τ_{SP} is a function of Z and c_m, we have to calculate for a given position of Q and a fixed value of Z_0, the local zenith angle Z of the sun at the centres of the successive layers along QP. For this, it is necessary to tabulate α shown in Fig. 1 for different values of c_m.

3.1. s, *the distance of the centre of the layer from the base of another layer in any direction*

From Fig. 1, we have

$$(a + c_m)^2 = s^2 + (a + b_n)^2 + 2s(a + b_n)\cos\theta'$$

On neglecting $c_m{}^2$ and $b_n{}^2$ in comparison with the other terms,

$$s^2 + 2s(a + b_n)\cos\theta' - 2a(c_m - b_n) = 0 \tag{22}$$

With the help of Equation (22), the values of s were tabulated for different values of c_m and $\theta' = 0°, 15°, 30°, 45°, 60°, 75°, 80°, 85°, 88°$ and $90°$ when the position of Q is at b_1, the ground level. From this table, it is easy to obtain the values of s corresponding to any b_n and θ' between 0° and 90° with sufficient accuracy. For positions of Q above the ground, when θ' can take values greater than 90°, QP can intercept some of the lower layers twice. This was appropriately allowed for in computing the path lengths for θ' between 90° and 180° at similar intervals. It is expected that the tabulated values of s are correct within 1 km. when s is small and within 2 km. when it is large.

3.2. Δs, *thickness of the layer in any direction*

Equation (22) was used to calculate the distance Δs between the bases of two consecutive layers for all the above-mentioned values of θ'. $\log_e \Delta s$ was tabulated for all values of c_m, b_n and θ' required in the calculation.

3.3. *Z, the local zenith distance of the sun for any position of P for a given* Z_0

In Fig. 1, the vertical through P (PR_1O) makes an angle a with the Z-axis. It can be represented by (a, ϕ') and Z is given by

$$\cos Z = \cos Z_0 \cos a + \sin Z_0 \sin a \cos \phi' \tag{23}$$

a can be determined from the relation

$$\sin a = \frac{s}{a + c_m} \sin \theta' \tag{24}$$

The values of $\sin a$ and $\cos a$ were tabulated for all the positions mentioned in 3·1 and used for the other similar positions as necessary.

When Z is greater than 90°, there is a limit below which P would not be illuminated by direct sunlight. Limiting values of cos Z for different values of c_m can be obtained from

$$\sin Z_s = \frac{a}{a + c_m} \tag{25}$$

With the help of Equation (24) tables of cos Z were prepared for Z_0 corresponding to 90°, 94°, 98°, 102° and 106° for all the values of θ' and b_n and at intervals of 15° for ϕ'.

3.4. τ_{SP}, *the equivalent optical path from outside the atmosphere to the point P which is at a height* c_m *above ground and for different values of* cos Z

Consider a point P situated at a height c_m in its vertical above the surface of the earth. Let the incident solar radiation make an angle Z with OP (Fig. 2). Let P′ be any point in SP, at a distance s from P and at a vertical height h from the ground. The density at P′ is given by

$$\rho = \rho_0 e^{-h/H}$$

and the equivalent optical path $\tau_{SP}(\cos Z, c_m)$ as defined by (1) is given by

$$\tau_{SP}(\cos Z, c_m) = \sigma\rho_0 \int_{\infty}^{P} e^{-h/H}\, ds \tag{26}$$

$$\sigma\rho_0 = \frac{8\pi^3}{3\lambda^4} \times \frac{(n_0^2 - 1)^2}{N_0} \times \frac{6(1 + d)}{6 - 7d} \tag{27}$$

where

λ = wave-length of the incident radiation
n_0 = refractive index of the air
N_0 = number of molecules per c.c. at the ground
ρ_0 = density of the air in gm. per c.c. at the ground.

From Fig. 2, we have,

$$(a + h)^2 = s^2 + (a + c_m)^2 + 2s\,(a + c_m) \cos Z$$

and neglecting c_m^2 and h^2 compared to the other terms, we have,

$$h = \frac{s^2}{2a} + \frac{(a + c_m) \cos Z}{a} s + c_m$$

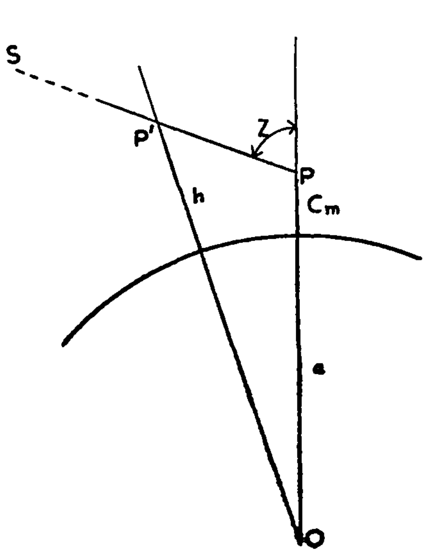

Fig. 2

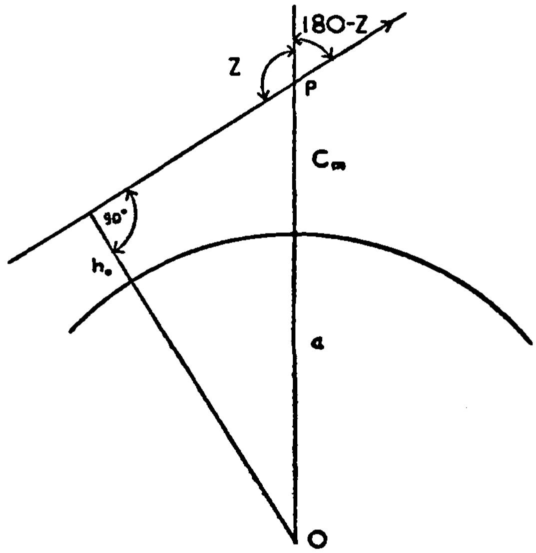

Fig. 3

On substituting this in Equation (26) and carrying out the integration, we have

$$\tau_{SP}(\cos Z, c_m) = \sigma\rho_0 \sqrt{\frac{\pi a H}{2}}\, e^{-c_m/H} \times e^{\frac{(a+c_m)^2 \cos^2 Z}{2aH}} \left[1 - \mathrm{Erf}\left\{\frac{(a + c_m) \cos Z}{\sqrt{2aH}}\right\}\right] \tag{28}$$

The function $\mathrm{Erf}(y)$ is tabulated in books of *Mathematical Tables* at regular intervals between 0 and 3 while for $y > 3$, we can use the standard expansion formula. It can be shown that for $\cos Z = 1$ and $c_m = 0$, Equation (28) reduces to

$$\tau_{SP}(1, 0) = \sigma\rho_0 H = \tau_1$$
$$= \text{the vertical optical path} \qquad (29)$$

After substituting $\sigma\rho_0$ by τ_1/H in Equation (28), the equation was used to tabulate $\tau_{SP}(\cos Z, O)/\tau_1$ for a number of intervals of cos Z between 0 and 1. From this, we can calculate τ_{SP} for any wave-length by selecting τ_1. The intervals are sufficiently numerous to obtain τ_{SP}/τ_1 for any cos Z within the accuracy required. For positive values of cos Z and c_m, $e^{-c_m/H}$ is the most important factor and

$$\tau_{SP}(\cos Z, c_m)/\tau_1 = \tau_{SP}(\cos Z, O)\, e^{-c_m/H}/\tau_1 \qquad (30)$$

For negative values of cos Z, the following method is used. From Fig. 3,

$$\frac{a + h_0}{a + c_m} = \sin Z$$

from which h_0 can be calculated for a given Z and c_m. Then

$$\frac{\tau_{SP}(\cos Z, c_m)}{\tau_1} = \frac{2\tau_{SP}(O, O)}{\tau_1} e^{-h/H} - \frac{\tau_{SP}\{\cos(180 - Z), c_m\}}{\tau_1} \qquad (31)$$

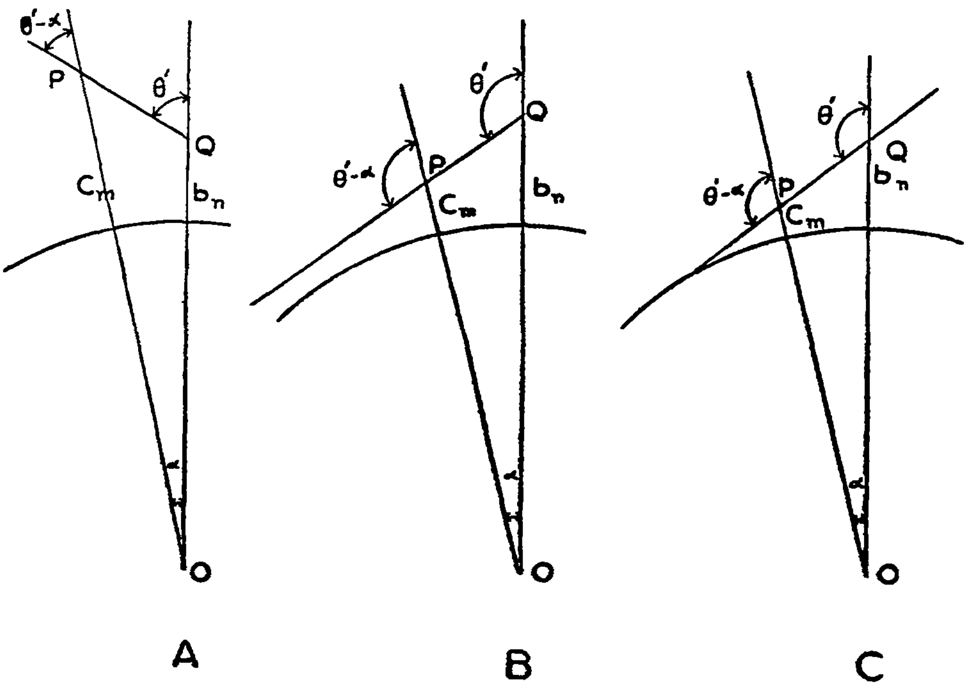

FIG. 4

Using Equation (31), $\tau_{SP}(\cos Z, c_m)/\tau_1$ were tabulated at regular intervals from zero to the shadow limit for different values of c_m from c_1 to c_{18}. For higher values of c_m the calculations were carried out whenever necessary.

3.5. τ_{PQ}, *equivalent optical path between any two points in the atmosphere*

From Figs. 4 A and B, we can write

$$\frac{\tau_{PQ}(\cos\theta', c_m \text{ to } b_n)}{\tau_1} = \frac{\tau_{SP}(\cos\theta', b_n)}{\tau_1} - \frac{\tau_{SP}\{\cos(\theta'-a), c_m\}}{\tau_1} \qquad (32)$$

For negative values of θ', for which PQ intersects the surface of the earth, the calculation of τ_{PQ} is similar to that indicated in Fig. 4 C.

IV. Intensity and Polarisation of the Zenith Sky

In this section the results of the computation of the intensity and polarisation of the primary and secondary radiations from the zenith sky during twilight for $\tau_1 = 0 \cdot 2$ corresponding to $\lambda = 4350$ A are given. The effect of adding a fixed intensity of night air-glow radiation with a polarisation of 4% as obtained from twilight observations is then discussed.

4.1. $R_{1n'}$, *primary scattered radiation received from any direction for different values of* Z_0

$R_{1n'}$ was calculated with the help of Equation (21). The summation extends over all the layers which lie in the sunlit part of the atmosphere. I_∞ was taken to be equal to unity, and $\sigma\rho_0 = \tau_1/H$ from Equation (29). Equation (21) shows that the part $e^{-\tau_{PQ}} e^{-c_m/H} \Delta s$ is independent of ϕ' and Z_0. An auxiliary table of $\{-\tau_{PQ} - c_m/H + \mathrm{Log}_e\, \Delta s\}$ for different values of b_n and $\tau_1 = 0 \cdot 2$ was prepared to reduce the work of computation.

When $R_{1n'}$ was computed for different values of θ' and ϕ', for $Z_0 = 90°$ and $b_n = b_1$ or b_2, it was noticed that for a fixed θ', the graph of $R_{1n'}$ against $\cos\phi'$ was nearly a straight line for values of θ' between 0° to 75° and between 100° to 180° (Fig. 5). It was slightly curved when θ' lay between 75° and 95°. Therefore, $R_{1n'}$ was obtained by linear interpolation after computing its value for $\cos\phi' = 1 \cdot 0, 0 \cdot 5, 0 \cdot 0, -0 \cdot 5$ and $-1 \cdot 0$ for a given b_n. This procedure was adopted when Z_0 was 90° and 94° and the whole sky more or less illuminated by direct solar radiation. For higher values of Z_0, $R_{1n'}$ was calculated individually for each ϕ' and θ' as only a small portion of the sky could then get direct sunshine.

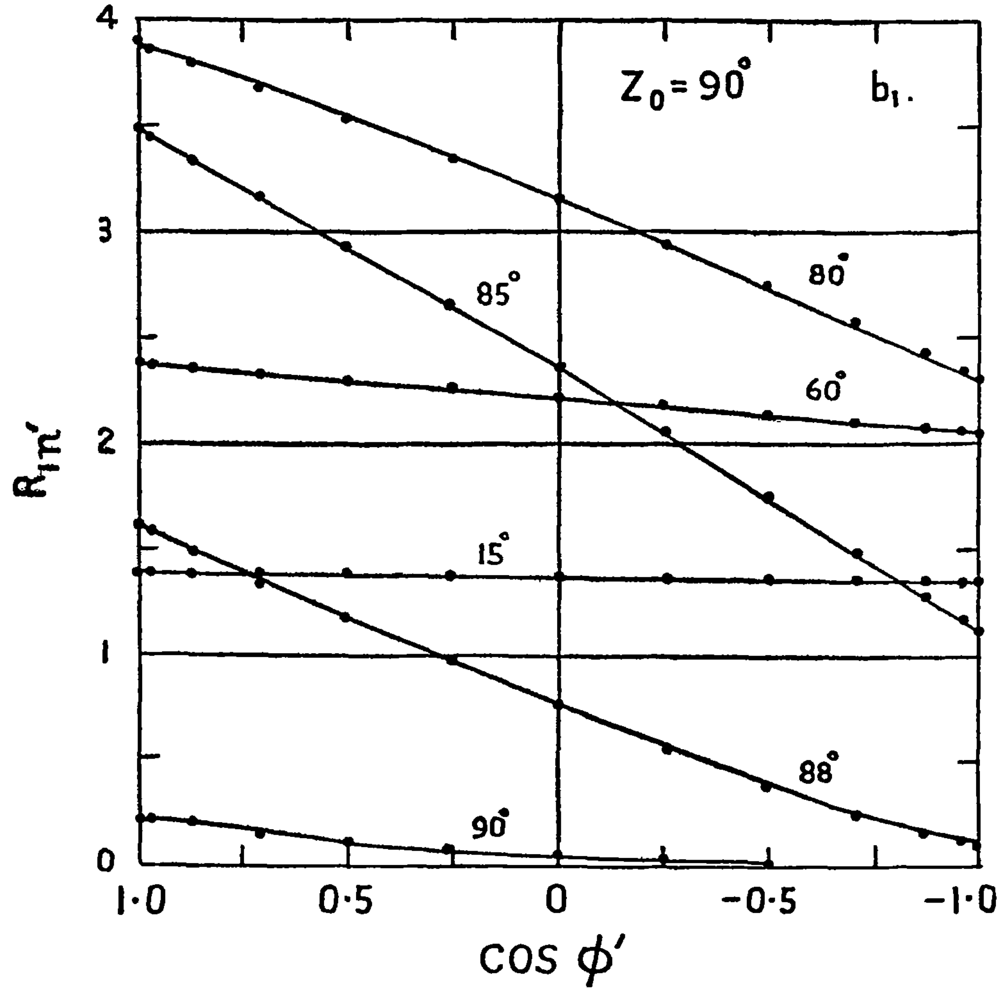

FIG. 5. Variation of the normal component of primary scattered light ($R_{1n'}$) with solar azimuth (cos ϕ') for different zenith angles of the sky from 15° to 90° as seen by an observer at ground level ($b_1 = 0$ km.). The sun is assumed to be on the observer's horizon ($Z_0 = 90°$).

The variation of the normal component of primary scattered radiation as received by the observer at the ground from different parts of the sky for Z_0 from 90° to 102° is shown in Fig. 6.

4.2. E_{2n} *and* E_{2t}: *Secondary emission from any point in the direction of observation*

Equation (17) can be rewritten as

$$\rho_0 E_{2n} = \frac{3\sigma\rho_0}{16\pi(1+\frac{1}{3}d)} \sum \sum [\{A_1 + KA_2\} R_{1n'} d\phi'] \sin\theta' . d\theta'$$

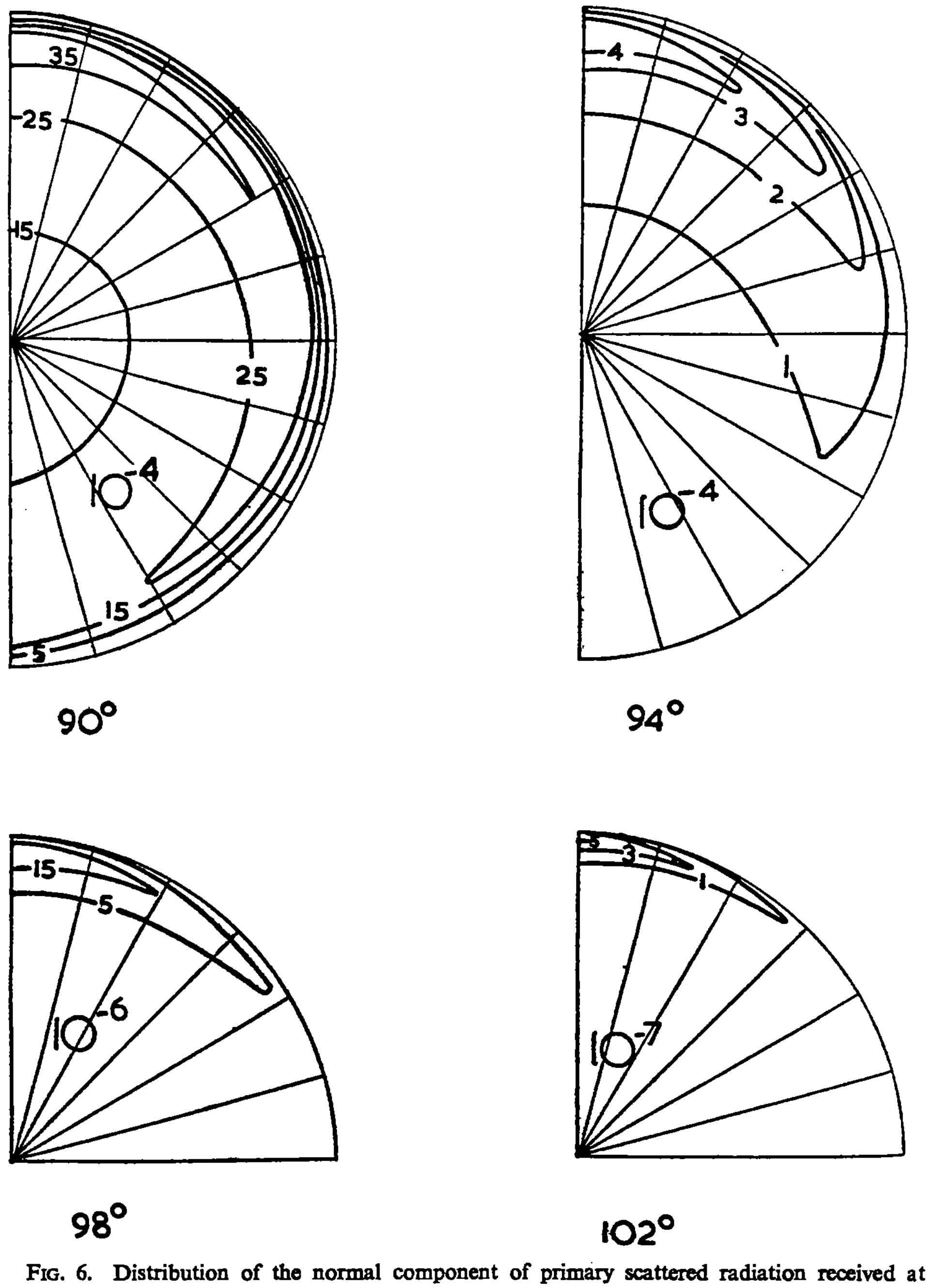

Fig. 6. Distribution of the normal component of primary scattered radiation received at the ground from different parts of the sky.

Knowing the values of $\{A_1 + KA_2\}$ and $R_{1n'}$ at definite intervals of θ' and ϕ' for different values of b_n and Z_0, further calculation was carried out in the following manner:

First, summation was carried out over ϕ', keeping θ' constant. $R_{1n'}$ was multiplied by the corresponding $\{A_1 + KA_2\}$, the arithmetic means of the consecutive products were then added and the sum multiplied by $d\phi' = 0 \cdot 5237$ radians corresponding to 30° interval. Symmetry about the principal plane gives the value for 30° from the tabulated values for 15° intervals.

For summation over θ', $\Sigma\,[\{A_1 + KA_2\}\, R_{1n'} d\phi']$ was multiplied by the corresponding value of sin θ', and the arithmetic means of consecutive terms were taken. $R_{1n'}$ includes the exponential $\exp(-\tau_{SP} - \tau_{PQ})$. These were then multiplied by corresponding intervals of $d\theta'$ in radians. The summation of the product multiplied by $3\sigma\,\rho_0/16\pi\,(1 + \frac{1}{2}d)$ gave the value of $\rho_0\, E_{2n}$ for the particular level b_n and Z_0 under consideration. The values of $\rho_0\, E_{2n}$ and $\rho_0 E_{2t}$ so obtained are given in Table I for different values of b_n and Z_0.

TABLE I

$\rho_0\, E_{2n}$ *for the observer's zenith for different values of* b_n *and* Z_0

b_n \ Z_0	90°	94°	98°	102°	106°
b_1	$0{\cdot}245\times10^{-4}$	$0{\cdot}143\times10^{-5}$	$0{\cdot}015\times10^{-6}$	$0{\cdot}013\times10^{-8}$	$0{\cdot}000\times10^{-10}$
b_2	0·339	0·199	0·032	0·051	0·025
b_3	0·445	0·262	0·062	0·133	0·117
b_4	0·535	0·326	0·101	0·287	0·383
b_5	0·584	0·406	0·162	0·605	1·037
b_6	0·587	0·491	0·237	1·040	1·994
b_7			0·295	1·389	2·769
b_8			0·311	1·507	3·048

$\rho_0\, E_{2t}$ for the observer's zenith for different values of b_n and Z_0

b_n \ Z_0	90°	94°	98°	102°	106°
b_1	$0{\cdot}077\times10^{-4}$	$0{\cdot}044\times10^{-5}$	$0{\cdot}004\times10^{-6}$	$0{\cdot}002\times10^{-8}$	$0{\cdot}000\times10^{-10}$
b_2	0·113	0·062	0·008	0·008	0·003
b_3	0·156	0·082	0·014	0·021	0·013
b_4	0·193	0·105	0·022	0·046	0·045
b_5	0·214	0·132	0·036	0·096	0·125
b_6	0·216	0·162	0·053	0·167	0·244
b_7			0·066	0·225	0·340
b_8			0·071	0·247	0·383

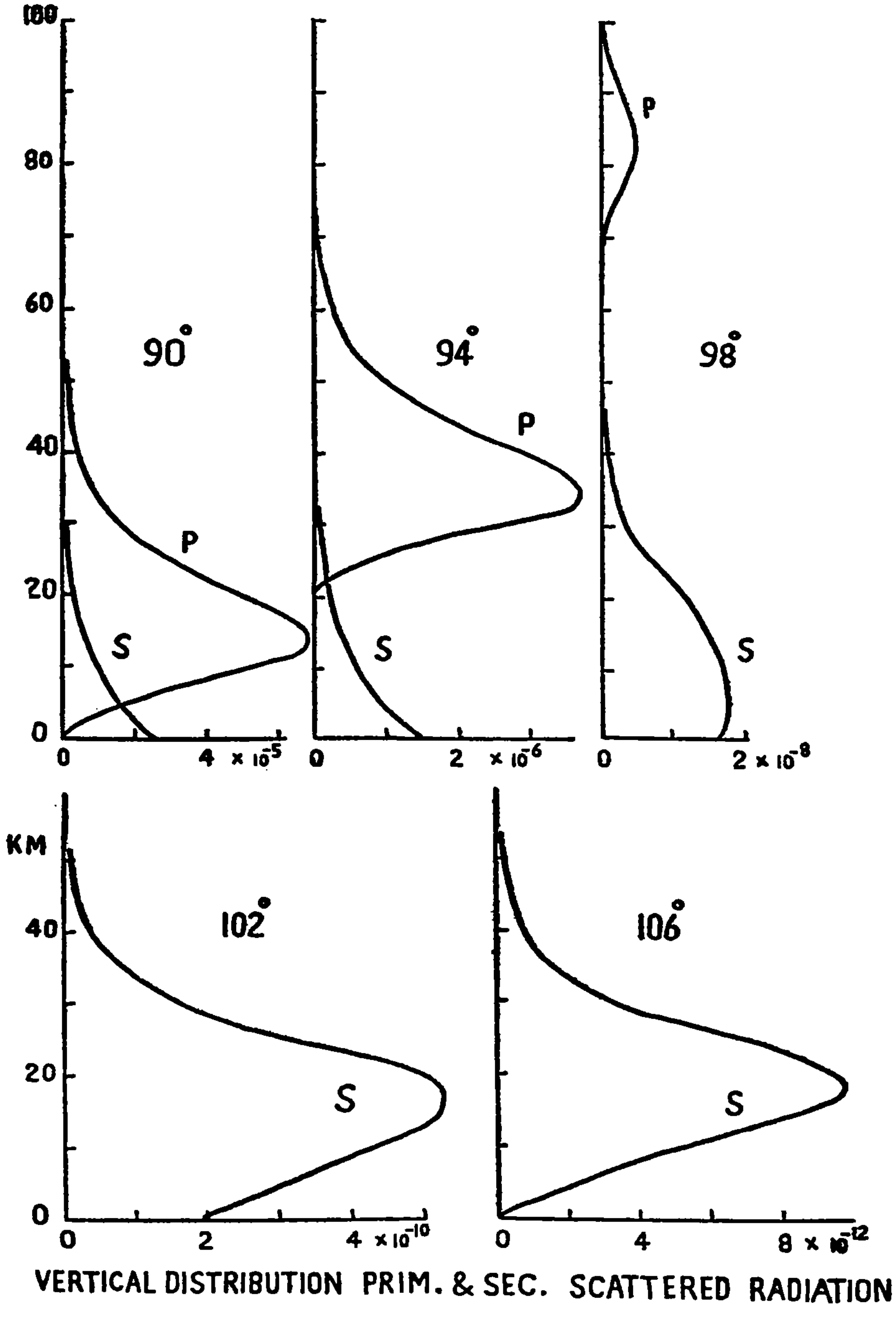

FIG. 7. Vertical distribution of primary and secondary scattered light from the zenith sky during twilight for solar zenith angles from 90° to 106°.

It will be seen from Table I that the computation has been stopped at b_6 for 90° and 94°. For heights greater than b_6, the value corresponding to b_6 has been used. A similar remark applies to heights greater than b_8 for 98°, 102° and 106°. This is justifiable because at these heights, the density becomes relatively small and the effective contribution to the light received by the observer becomes negligible (see Fig. 7).

4.3. *R_{2n} and R_{2t}: Normal and transverse components of the total secondary scattered light as received by the observer at the ground from his zenith*

Equation (19) can be rewritten as

$$R_{2n} = \Sigma \rho_0 E_{2n} e^{-\tau_{QR_0}} e^{-C_m/H} \Delta s \tag{33}$$

the summation extending over all the layers above the point of observation. $\Delta s = 4$ km. for $\theta = 0°$, $\phi = 0°$. τ_{QR_0} is the same as τ_{PQ} for $\theta' = 0°$ and $b_n = b_1$ when the observer is situated at ground level and the direction of observation is along his zenith. The value of $\rho_0 E_{2n}$ is the arithmetic mean of two successive values of b_n given in Table I. The vertical distribution of primary and secondary scattered radiation from the zenith sky for different solar angles are plotted in Fig. 7.

The values of R_{2n} and R_{2t} are given in Table II along with R_{1n}, R_{1t}, P_1 and P_2 where P_1, P_2 are the percentage polarisations of primary and secondary scattered light. P is defined by

$$P = \frac{R_n - R_t}{R_n + R_t} \times 100 \tag{34}$$

TABLE II

Intensity and polarisation of the primary and secondary scattered radiations from the zenith sky

Z_0	R_{1n}	R_{1t}	P_1 %	R_{2n}	R_{2t}	P_2 %
90	$1{\cdot}30\times10^{-3}$	$0{\cdot}052\times10^{-3}$	92·3	$2{\cdot}43\times10^{-4}$	$0{\cdot}84\times10^{-4}$	49
94	$6{\cdot}93\times10^{-5}$	$0{\cdot}31\times10^{-5}$	91·4	$1{\cdot}52\times10^{-5}$	$0{\cdot}48\times10^{-5}$	52
98	$9{\cdot}0\times10^{-8}$	$0{\cdot}5\times10^{-8}$	89	$4{\cdot}13\times10^{-7}$	$0{\cdot}94\times10^{-7}$	63
102	..	..	..	$1{\cdot}26\times10^{-8}$	$0{\cdot}20\times10^{-8}$	72
106	..	..	..	$1{\cdot}95\times10^{-10}$	$0{\cdot}24\times10^{-10}$	78

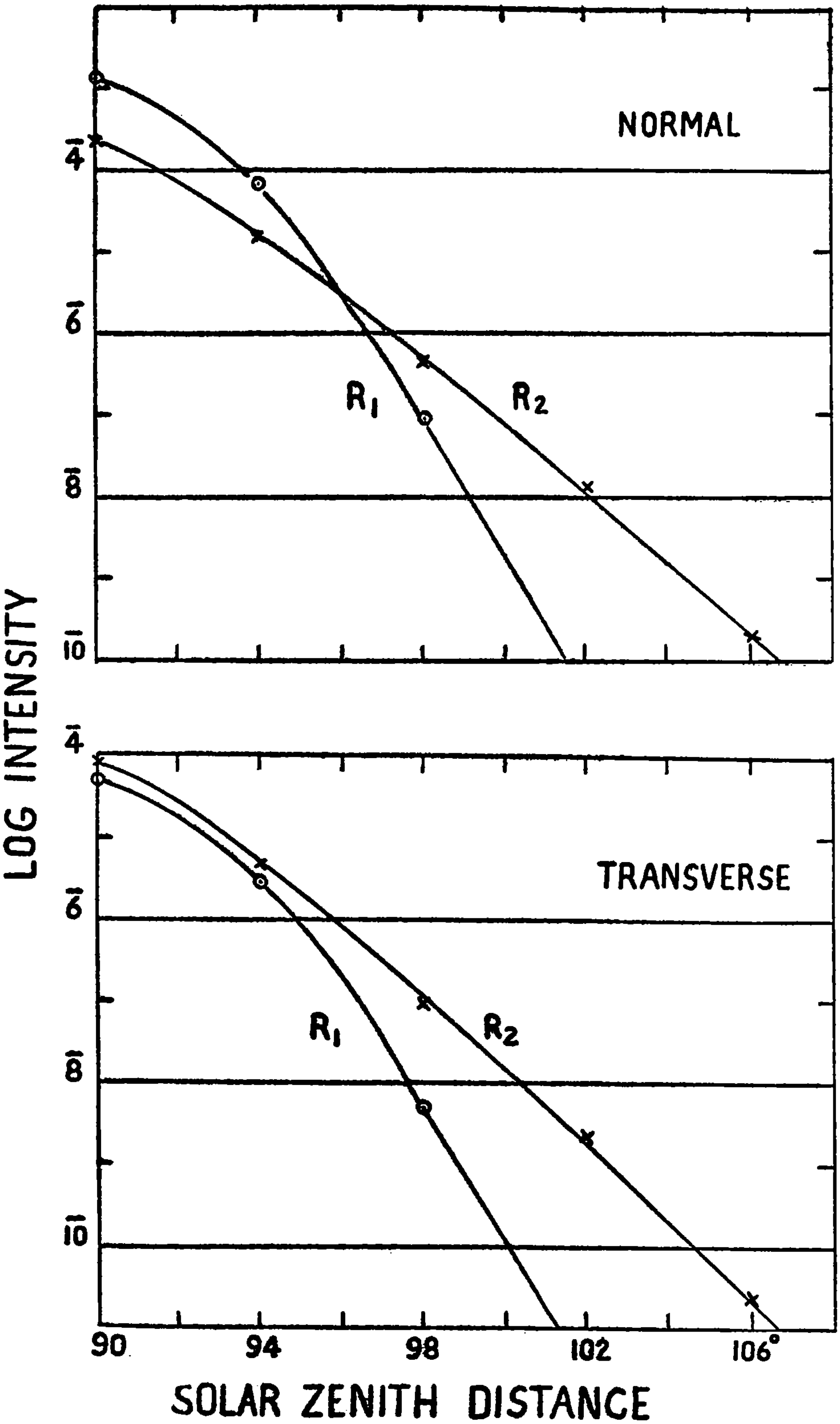

FIG. 8. Variation of the normal and transverse components of primary and secondary scattered light from the zenith sky during twilight.

4.4. *Variation of the intensity and polarisation of the zenith sky during twilight*

Figure 8 gives the variation of R_{1n}, R_{1t}, R_{2n} and R_{2t} with Z_0. Smooth curves were drawn from the values given in Table II and from them, the values were read out at each 1° interval to calculate the intensities and polarisations of the zenith sky at different zenith angles of the sun.

Figure 9 shows the variation with Z_0, of (*a*) the primary scattered radiation R_1, (*b*) the primary and secondary scattered radiations together, $R_1 + R_2$, (*c*) $R_1 + R_2 + R_0$ when R_0 is the background night air-glow radiation assumed to be constant at $1 \cdot 92 \times 10^{-9}$ and (*d*) the observed intensity

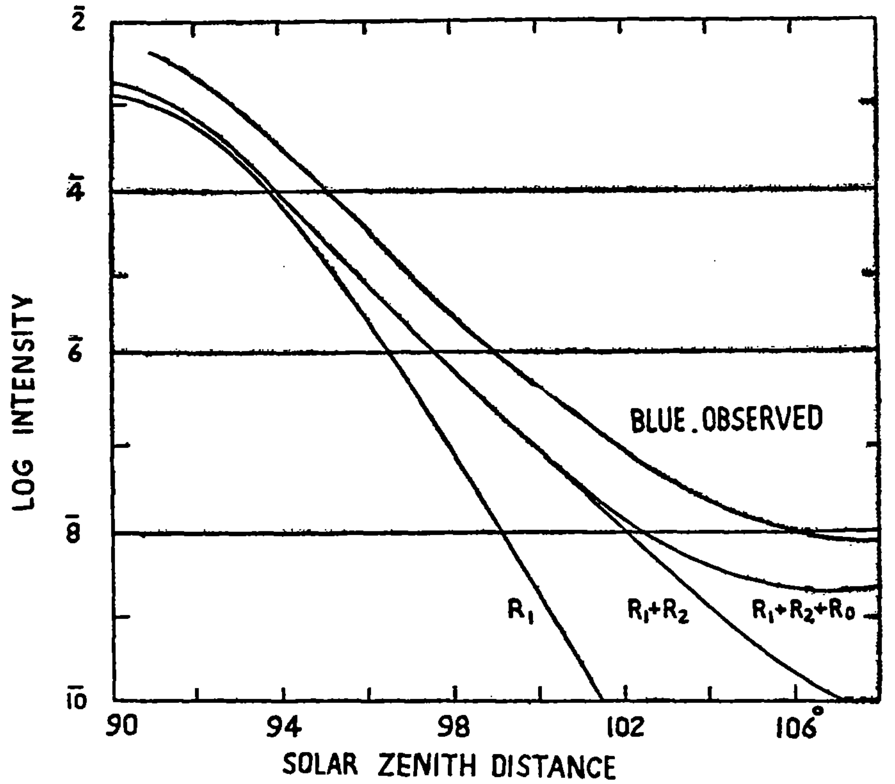

FIG. 9. Variation of the intensity of the zenith sky during twilight.

R_1 .. Primary scattering alone.

$R_1 + R_2$ .. Primary *plus* secondary scattering.

$R_1 + R_2 + R_0$.. $R_1 + R_2$ *plus* background night air-glow of constant intensity.

of the zenith sky for $\lambda = 4{,}500$ A during evening twilight as observed at Mount Abu. The magnitude of R_0 was fixed from observations of the zenith sky when the sun was more than 18° below the horizon.

It can be seen from the figure that the secondary scattered radiation becomes more and more important after 95°. Between 98° and 102°, the light received by the observer is mainly secondary scattered radiation. Afterwards, the night air-glow becomes comparable in intensity to secondary scattered light, and by 106°, practically only night sky emission remains as the factor contributing to the zenith sky intensity.

In Fig. 10 are given the curves of polarisation of the zenith sky when the different contributions are considered singly or jointly. The curve giving the polarisation of the primary scattered light shows that it is 92% at sunset and decreases to 88% at 100°. On the contrary, S representing the polarisation of the secondary scattered light shows an increase from 48% at sunset to 79% at 106°. Adding the normal and transverse components of the two radiations from the zenith sky and calculating the effective polarisation, the polarisation gets reduced to 84% at sunset. After 94°, the secondary scattered radiation becomes relatively more important and the polarisation shows a rapid fall; after 98°, P becomes unimportant and P + S follows S.

If night sky radiation of intensities $R_{0n} = 1 \cdot 00 \times 10^{-9}$ and $R_{0t} = 0 \cdot 92 \times 10^{-9}$ be added to $R_{1n} + R_{2n}$ and $R_{1t} + R_{2t}$ respectively, and the polarisation recalculated (Curve P + S + N), the curve gradually changes its course when the zenith distance of the sun increases beyond 99°, and the change becomes rapid after 102°. When Z is greater than 108°, night conditions get fully established.

When the calculated polarisation curve is compared with that obtained by observation, it is seen that while there is agreement in general features, there are some important differences. The observed values of polarisation are markedly smaller. The transitions are sharper in the observed curve than in the calculated one.*

This is probably due to the following causes:—

(1) The effect of dust in the atmosphere and of tertiary and higher orders of scattering have been neglected. Inclusion of these in the calculation will decrease the polarisation.

(2) The density of the atmosphere has been assumed to decrease exponentially with height with a scale height of 7 km. Actually, there are well marked stratifications in the atmosphere and the decrease of density with height is not a simple exponential. The difference

* Recent observations of polarisation at Mount Abu with a better type of polaroid have shown 80% polarisation at sunset and 55 to 60% between 8 and 12° solar depression.

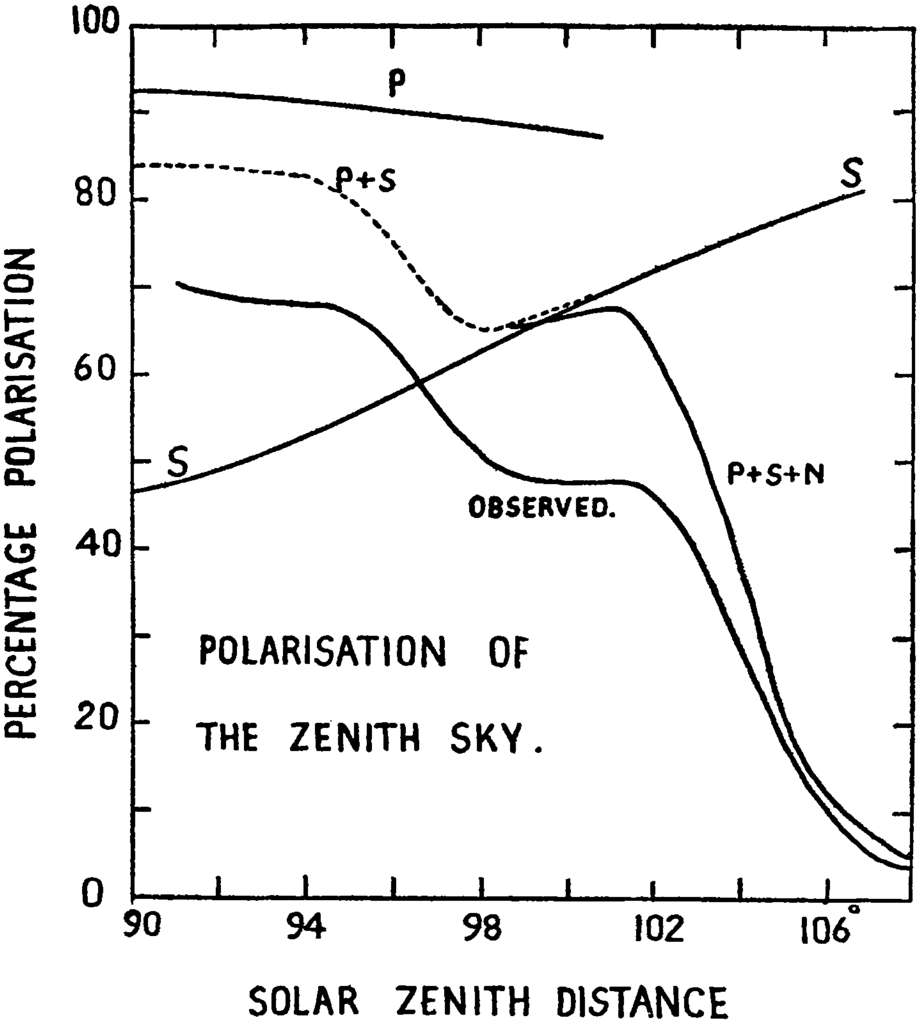

FIG. 10. Polarisation of the zenith sky during twilight for different zenith distances of the sun.

P	..	Percentage polarisation of primary scattered light.
S	..	Percentage polarisation of secondary scattered light.
P + S	..	Effective percentage polarisation of primary *plus* secondary scattered light.
P + S + N	..	Total effective polarisation when night air-glow of constant intensity and 4% polarisation is added to primary *plus* secondary scattered light.
Observed	..	Observed zenith sky polarisation at Mount Abu.

between the courses of the observed and calculated curves between 94° and 98° can be related to the existence of the warm ozone layer between 30 and 60 km. An attempt is being made to remedy these defects in the theory.

V. POLARISATION OF THE SKY AT POINTS 30° FROM THE ZENITH AND IN THE PRINCIPAL PLANE OF THE SUN

In Part I, we also presented the observations of polarisation during twilight from two directions in the sky other than zenith, (1) at 30° from the zenith on the sunside $\theta = 30°$, $\phi = 0°$ and (2) at 30° from the zenith on the anti-sunside, $\theta = 30°$, $\phi = 180°$. These curves while showing the general features of the zenith polarisation curve, show some differences. In order to understand this, calculations have also been made of the polarisation in these two directions. They are plotted in Fig. 11.

The polarisation curves for the sunside show that the polarisation of primary scattered light (P) increases with Z_0 and so also the polarisation of secondary scattered light (S). However, the secondary scattered radiation is polarised to a much smaller extent than the primary and hence the resultant polarisation P + S, increases with Z_0 in the beginning when the primary scattered radiation is prominent and decreases afterwards when $Z_0 = 94 \cdot 5°$. For $Z_0 = 100°$, the primary scattered radiation is negligible and P + S practically coincides with S. On adding the night sky radiation, the P + S curve deviates from the S curve at 100°, and by 102° a sharp fall occurs.

On the anti-sun side, the polarisation of P shows a fall with Z_0 and the rate of increase of S is much smaller than on the side of the sun. This causes a slight fall of polarisation in the beginning and a comparative flat region between 98° and 102°.

VI. SUMMARY

The formulæ for the intensity of the secondary scattered light from the sky as developed by Chapman and Hammad for a plane-parallel infinite atmosphere of defined optical thickness have been modified so as to deal with the twilight problem in which the curvature of the atmosphere is of fundamental importance. Calculations have been made of the intensity and polarisation of the light received from the zenith sky for different values of the sun's zenith distance from 90° to 107° and for a radiation for which the optical thickness of the atmosphere is 0·2. For 0° to 5° solar depression, the primary scattering is predominant; as the angle increases, the secondary scattered light becomes more and more important and when the sun's depression is 8° to 12°, it is the principal contributing factor. Afterwards, the night air-glow becomes comparable in intensity and when the solar depression is 17° to 18°, only the air-glow radiation remains. The calculated values of intensity and polarisation are compared with the observational data collected at Mount Abu.

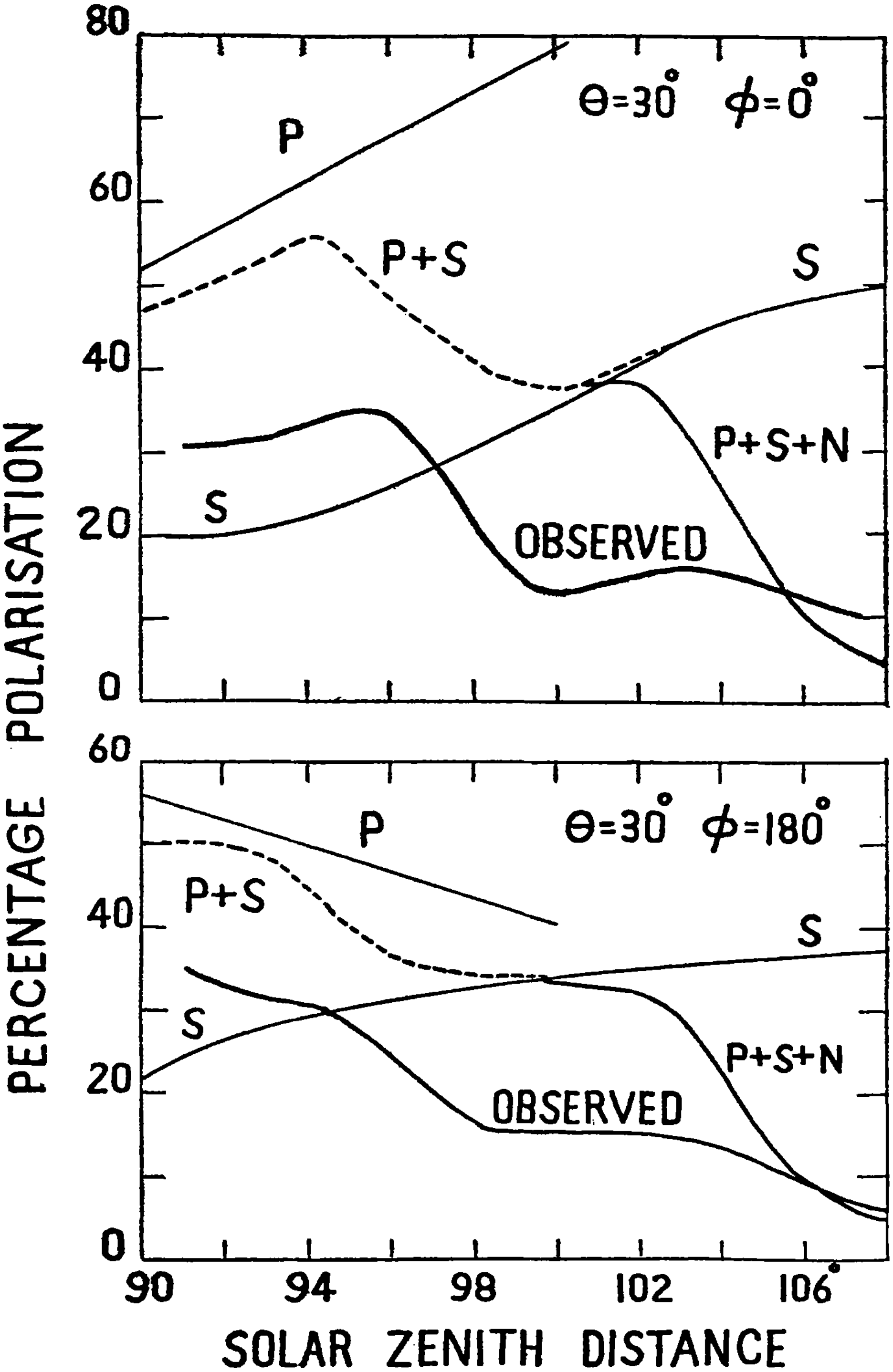

FIG. 11. Polarisation of the sky at points 30° from the zenith in the principal plane of the sun.

P	..	Percentage polarisation of primary scattered light.
S	..	Percentage polarisation of secondary scattered light.
P + S	..	Effective percentage polarisation of primary *plus* secondary scattered light.
P + S + N	..	Total effective percentage polarisation when night air-glow of constant intensity and 4% polarisation is added to primary *plus* secondary scattered light.
Observed	..	Observed sky polarisation at Mount Abu.

The author is grateful to the Council of Scientific and Industrial Research for the award of a Research Assistantship during the course of this study. He acknowledges with pleasure the help given by Shri V. L. Bhatt, M.SC., in preparing some of the diagrams. Finally, the author takes this opportunity to express his indebtedness to Prof. K. R. Ramanathan, for suggesting the problem and valuable guidance.

REFERENCES

1. Dave, J. V. and Ramanathan, K. R. *Proc. Ind. Acad. Sci.*, 1956, **43 A**, 67.
2. Hulburt, E. O. .. *Journ. Opt. Soc. America*, 1938, **28**, 227.
3. Robley, R. .. *Annales de Geophysique*, 1952, **8**, 1.
4. Chandrasekhar, S. .. *Radiative Transfer*, The International Series of Monographs on Physics, Clarendon Press, Oxford, 1950.
5. Hammad, A. and Chapman, S. .. *Phil. Mag.*, 1939, **28**, 99.
6. Hammad, A. .. *Astrophys. Journ.*, 1948, **108**, 338.
7. Link, F. and Sekera, Z. .. *Publ. Obs. Nat., Prague*, 1940, **14**, 1.
8. Chapman, S. .. *Proc. Phys. Soc.*, 1931, **43**, 483.
9. ——— .. *Ibid.*, 1953, **66 B**, 710.